A Nonlinear Switched Observer with Projected State Estimates for Diesel Engine Emissions Reduction

Philip James McCarthy Christopher Nielsen Stephen L. Smith

***Abstract*— This paper presents an exponentially converging nonlinear switched observer for diesel selective catalytic reduction (SCR) nitrogen oxide (NO_x) aftertreatment systems using only NO_x measurements. The state of the SCR system is shown to evolve in a physically meaningful positively invariant set. A state estimator is designed using a continuous-time observer, a switching law, and a projection that ensures the estimates are in the positively invariant set. The convergence rate of the estimates to the SCR states has the same bound as the corresponding continuous-time observer.**

I. INTRODUCTION

One of the most important aspects of modern air quality management is the control of diesel engine emissions [1]. Some of the key pollutants produced by diesel engines are nitrogen oxides (NO_x). The USA, EU, and Japan have strict regulations restricting NO_x emissions of diesel engines, particularly the state of California, whose maximum emissions limit is 80% lower than the EU's for light-duty engines [1]. Selective catalytic reduction (SCR) has been identified as one of the most promising methods of NO_x emissions reduction [2]. The reduction is achieved by mixing ammonia (NH_3) with the NO_x inside a reactor, located downstream from the engine. However, because of the toxicity of NH_3, urea is injected instead, which produces NH_3 through a series of reactions [2]. In some regions, such as the USA, the toxic NH_3 "slip", i.e., unreacted NH_3 that does not mix with the exhaust and exits the SCR reactor, is not regulated, but self-imposed limits of 10 ppm in steady-state and 20 ppm during transients have been adopted [3]. This is the central SCR control problem, the goal of which is to satisfy two dichotomous criteria: simultaneously minimize both NO_x emissions and NH_3 slip. Injecting more urea reduces NO_x, but also increases NH_3 slip.

The SCR control problem is addressed using state feedback control schemes, such as in [3], [4], [5], [6]. The key values used for SCR state feedback control are NO_x concentration, NH_3 concentration, and NH_3 coverage; the percentage of the catalyst's surface that is covered with NH_3. Since NH_3 slip is not regulated in some regions, combined with the high cost of NH_3 and NO_x sensors, commercial SCR reactors are often not equipped with NH_3 sensors [3]. Also, the NH_3 coverage ratio θ cannot be measured; it must be inferred from measured values such as temperature, NO_x concentration, and NH_3 concentration. Since these two key values in SCR operation and control are not known via measurement, they must be deduced using an observer. Despite the fact that commercial SCR units are often not equipped with NH_3 sensors, much research in this area is conducted under the assumption that these sensors are available [3], [7], [8], [9], [10].

Sliding mode estimation strategies are used in [7] and [8], the former estimating the NH_3 coverage and the latter estimating the mid-catalyst NH_3 concentration. In [6] a linear-parameter-varying observer is designed to estimate the NH_3 coverage, using only a NO_x sensor. The extended Kalman filter was used in [9] to estimate NO, NO_2, and the NH_3 coverage, and in [10] to estimate the NH_3 coverage.

In this paper, we propose a nonlinear observer based on that in [11] with saturated state estimates, so as to keep the estimates within a physically meaningful positively invariant set, thereby bounding the estimation error. The saturation effect is implemented using state-dependent switched dynamics. If the saturated dynamics interfere with convergence, the observer's dynamics and estimates switch to those of the underlying observer, but outputting a projected version of its estimates to the controller. The proposed observer is shown to be exponentially stable, and to have the same convergence rate bound as that in [11].

We assume that NO_x sensors at both the inlet and outlet of the SCR are available. The observer estimates the concentrations of NO_x and NH_3, as well as the NH_3 coverage ratio θ along the length of the catalyst.

Our contributions are: 1) we show that a simplified standard SCR system [4] is observable, and that the nonlinear observer in [11] can be used; 2) we note that the state estimates are capable of taking on physically meaningless values, thus we introduce switched dynamics and projections to the observer and analyze their effect on stability and convergence; 3) we illustrate our results in simulation.

II. BACKGROUND

In this section we introduce our notation, the class of systems to which our observer applies, and the SCR model.

A. Notation

Given a set $\Omega \subseteq \mathbb{R}^n$, let $\bar{\Omega}$ be its closure, and $\partial\Omega$ be its boundary. Given a vector $x \in \mathbb{R}^n$ and a set $\Omega \subset \mathbb{R}^n$, let $\overline{x}(\Omega)$ [$\underline{x}(\Omega)$] be the vector whose elements comprise the upper [lower] bounds of the intervals defining Ω, and $x^\top$ be its transpose. Let $\mathbf{0}_n \in \mathbb{R}^n$ denote the vector of all zeros. Given a C^1 mapping $\phi : \mathbb{R}^n \to \mathbb{R}^m$ let $d\phi(x)$ be its Jacobian evaluated at $x \in \mathbb{R}^n$. Given a rational function $g : \mathbb{R}^n \to \mathbb{R}$,

This research is partially supported by the Natural Sciences and Engineering Research Council of Canada (NSERC).

The authors are with the Dept. of Electrical and Computer Engineering, University of Waterloo, Waterloo ON, N2L 3G1 Canada. {philip.mccarthy;cnielsen;stephen.smith}@uwaterloo.ca

let num(g) be its numerator. Lastly, given a smooth function $h : \mathbb{R}^n \to \mathbb{R}$ and a smooth vector field $f : \mathbb{R}^n \to \mathbb{R}^n$, let $L_f^k h(x)$ be the k-times repeated Lie derivative of $h(x)$ in the direction of the vector field $f(x)$.

B. Selective Catalytic Reduction Reactor Model

To model the SCR system, we adopt a multi-cell modelling strategy, as described in [5]. The SCR volume is divided into N cells connected in series. The block diagram between adjacent cells is illustrated in Figure 1. The concentrations

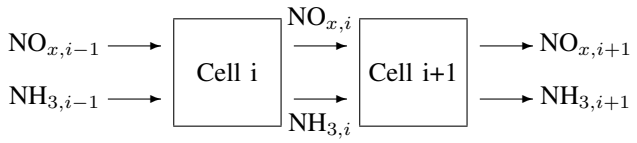

Fig. 1. Propagation of dynamics between adjacent cells

of NO_x and NH_3 are the inputs and outputs of each cell. Every cell has identical dynamics, with the output of cell i treated as the input to cell $i+1$. In addition to NO_x and NH_3, each cell has its own NH_3 coverage, denoted by θ, that has no inter-cell dynamic coupling. Together, the NH_3 coverage θ, outgoing NO_x, and outgoing NH_3 compose the states of an individual cell. The NO_x emissions and NH_3 slip of the overall system are the respective concentrations of the Nth cell. Since NH_3 sensors are prohibitively expensive and θ cannot be measured, $NO_{x,N}$ is the only output that can be reliably measured in a non-laboratory scenario.

For each cell, the model used in this paper is based on that used in [4]. Denote the state of the ith cell by $x_i \coloneqq \begin{bmatrix} x_{1,i} & x_{2,i} & x_{3,i} \end{bmatrix}^\top \coloneqq \begin{bmatrix} C_{\mathrm{NO},i} & \theta_i & C_{\mathrm{NH}_3,i} \end{bmatrix}^\top$.

TABLE I
PHYSICAL INTERPRETATION OF SYSTEM PARAMETERS

Parameter	Chemical/Physical Symbol [4]	Meaning
α	$\left({}^{F}/_{V}\right)/N$	volumetric flow rate over catalyst volume in a single cell
β	${}^{1}/_{\sigma}$	inverse of NH_3 storage capacity
$r_{1,i}$	$\sigma R_{red,i}$	normalized reduction reaction rate
$r_{2,i}$	$\sigma R_{ox,i}$	normalized oxidation reaction rate
$r_{3,i}$	$\sigma R_{des,i}$	normalized desorption reaction rate
$r_{4,i}$	$\sigma R_{ads,i}$	normalized adsorption reaction rate

For $i = 2, \ldots, N$, the cell dynamics are

$$\begin{aligned}
\dot{x}_{1,i} &= -r_{1,i}x_{1,i}x_{2,i} - \alpha(x_{1,i} - x_{1,i-1}) \\
\dot{x}_{2,i} &= -\beta x_{2,i}(r_{2,i} + r_{1,i}x_{1,i} + r_{3,i}) - \beta(x_{3,i}r_{4,i}(x_{2,i} - 1)) \\
\dot{x}_{3,i} &= r_{3,i}x_{2,i} + r_{4,i}x_{3,i}(x_{2,i} - 1) - \alpha(x_{3,i} - x_{3,i-1}),
\end{aligned} \tag{1}$$

where $r_{1,i}$, $r_{2,i}$, $r_{3,i}$, β, and α are physical constants (when temperature is in steady-state) described in Table I. Note that in the expression for $\dot{x}_{1,i}$ we neglect the term $r_{2,i}x_{2,i}$. Under reasonable operating conditions, i.e., NO_x concentrations on the order of 10^{-3} mol/m^3 and temperatures below $400°$C, we have $r_{2,i}x_{2,i} \ll r_{1,i}x_{1,i}x_{2,i}$ [4]. It is verified in [4] that, in practice, the neglected term does not affect observability.

The dynamics of the first cell, i.e., $i = 1$, are similar to (1), except that since there is no cell zero, the relevant states are replaced by the control input and a measured disturbance. The control input $u \in \mathbb{R}_{\geq 0}$ is the concentration of NH_3 from a urea pump and the measured disturbance $d \in \mathbb{R}_{\geq 0}$ is the concentration of NO_x emissions from a diesel engine, which is proportional to the load. The model of cell 1 is therefore

$$\begin{aligned}
\dot{x}_{1,1} &= -r_{1,1}x_{1,1}x_{2,1} - \alpha(x_{1,1} - d) \\
\dot{x}_{2,1} &= -\beta x_{2,1}(r_{2,1} + r_{1,1}x_{1,1} + r_{3,1}) - \beta(x_{3,1}r_{4,1}(x_{2,1} - 1)) \\
\dot{x}_{3,1} &= r_{3,1}x_{2,1} + r_{4,1}x_{3,1}(x_{2,1} - 1) - \alpha(x_{3,1} - u).
\end{aligned} \tag{2}$$

Stacking the states of each cell in reverse order, i.e., cell N on top, cell 1 on the bottom, we obtain the overall state vector $x = \begin{bmatrix} x_N & \cdots & x_1 \end{bmatrix}^\top \in \mathbb{R}^{3N}$. Combining (1) and (2) and assuming that the only measured output is the NO_x concentration of cell N, the overall state space model is

$$\dot{x} = f(x) + \begin{bmatrix} B_d & B_u \end{bmatrix} \begin{bmatrix} d & u \end{bmatrix}^\top, \quad y = h(x) = x_{1,N}, \tag{3}$$

where $B_d = \begin{bmatrix} \mathbf{0}_{n-3} & \alpha & 0 & 0 \end{bmatrix}^\top$, $B_u = \begin{bmatrix} \mathbf{0}_{n-1} & \alpha \end{bmatrix}^\top$, and $n \coloneqq 3N$. The drift vector field $f : \mathbb{R}^n \to \mathbb{R}^n$ is smooth and $\begin{bmatrix} B_d & B_u \end{bmatrix} =: B \in \mathbb{R}^{n \times 2}$ is constant. System (3) is a special case of the class of control affine systems, i.e.,

$$\dot{x} = f(x) + g(x)u, \qquad y = h(x), \tag{4}$$

with $g(x) = B$.

We assume that the engine has been operating at constant load (constant d) long enough that the temperature along the length of the catalyst is constant, and that the steady-state values of the parameters in Table I are known for a given d.

III. EXTENDED LUENBERGER OBSERVER

Before characterizing our proposed switched observer in Section V, we introduce the continuous-time observer which serves as its foundation.

The observer proposed in [11] is obtained by first expressing (4) in a canonical form, which is realized via the candidate diffeomorphism $T : \Omega \to T(\Omega)$, $x \mapsto \begin{bmatrix} h(x) & L_f h(x) & \cdots & L_f^{n-1}h(x) \end{bmatrix}^\top$, where Ω is a subset of $\mathbb{R}^n$. If the the assumptions of [11], summarized below, hold, then the transformed system is of the form

$$\begin{aligned}
\dot{z} &= \begin{bmatrix} z_2 & z_3 & \cdots & z_n & \varphi(z) \end{bmatrix}^\top \\
&\quad + \begin{bmatrix} g_1(z_1) & g_2(z_1, z_2) & \cdots & g_n(z_1, \ldots, z_n) \end{bmatrix}^\top u \\
&=: F(z) + G(z)u \\
y &= \left(h \circ T^{-1}\right)(z) = z_1 = Cz,
\end{aligned} \tag{5}$$

where $z \in \mathbb{R}^n$ is the vector of states in the transformed coordinates, $F : \mathbb{R}^n \to \mathbb{R}^n$ is the drift vector field in the transformed coordinates, and $G : \mathbb{R}^n \to \mathbb{R}^{n \times m}$ is the vector field of the input dynamics in the transformed coordinates. The observer, expressed in z-coordinates, is

$$\dot{\hat{z}} = F(\hat{z}) + G(\hat{z})u - S^{-1}(\Theta)C^\top(C\hat{z} - y), \tag{6}$$

where $\Theta \in \mathbb{R}_{>0}$ is a gain, $S(\Theta) \in \mathbb{R}^{n \times n}$ is the unique, positive definite solution to the Sylvester equation $\left(\Theta I + A^\top\right) S(\Theta) + S(\Theta)A = C^\top C$, and the pair (A, C) is in observable canonical form. An appealing quality of this observer is its structural simplicity; it is the original dynamics

of the system with the addition of an error term. The observer is implemented by converting (6) back to x-coordinates

$$\dot{\hat{x}}(t) = f(\hat{x}) + g(\hat{x})u - \frac{\partial}{\partial z}T^{-1}(z)\Big|_{z=T(\hat{x})} S(\Theta)^{-1}C^{\top}(\hat{x}_1 - y). \tag{7}$$

The applicability of the observer from [11] is contingent upon four hypotheses.

- H1 T is a diffeomorphism from Ω onto $T(\Omega)$.
- H2 The function $\varphi(z)$ in (5) can be extended from Ω to all of $\mathbb{R}^n$ by a C^∞ function, globally Lipschitz on $\mathbb{R}^n$.
- H3 System (4) is observable for any bounded input.
- H4 $g_i(z), i = 1, \ldots, n$ in (5) is globally Lipschitz.

We show in Sections IV and V-A that the SCR model satisfies these assumptions on an appropriately defined compact set Ω.

IV. MODEL ANALYSIS

In this section, the SCR system (3) is shown to evolve only within a positively invariant subset $\Omega \subset \mathbb{R}^n$. We therefore are interested in solving the observation problem only on this set, hereinafter referred to as the observation subset. We characterize the observation subset Ω and address the validity of H1 and H4 on the SCR system (3).

A. Observation Subset

Our goal is to define the observation subset Ω such that it is positively invariant under the dynamics of (3) and such that all $x \in \Omega$ make physical sense. The concentration of NO_x emissions cannot exceed the maximum NO_x output of a given engine, $d_{max} > 0$. The NH_3 slip is constrained by $NH_{3,max}$. As a ratio, θ takes values between 0 and 1. The natural choice of the observation subset is therefore

$$\begin{aligned}\Omega \coloneqq \{x \in \mathbb{R}^n : x_{1,i} \in (0, d_{max}), x_{2,i} \in (0,1),\\ x_{3,i} \in (0, \mathrm{NH}_{3,max,i}),\ i = 1, \ldots, N\}.\end{aligned} \tag{8}$$

We first characterize the value of $\mathrm{NH}_{3,max,i}$ that ensures Ω is positively invariant for (3).

Proposition IV.1. *Let*

$$\mathrm{NH}_{3,max,i} \coloneqq \frac{1}{\alpha}\sum_{k=1}^{i} r_{3,k} + u_{max}. \tag{9}$$

If $x(0) \in \Omega$ as defined in (8)*, then $x_{3,i} < \mathrm{NH}_{3,max,i}, \forall t \geq 0$.*

Proof. A function $f : \mathbb{R} \to \mathbb{R}$ is either unbounded as its argument tends to $\pm\infty$, or its extrema are at critical points. We first examine $\dot{x}_{3,i}$ as $x_{3,i} \to \pm\infty$

$$\lim_{x_{3,i}\to\pm\infty} \dot{x}_{3,i} = r_{4,i}x_{3,i}(x_{2,i} - 1) - \alpha x_{3,i}. \tag{10}$$

On the closure of Ω, $\bar{\Omega}$, $x_{2,i} \in [0,1]$. Therefore, if $x_{3,i}$ is positive [negative], then (10) is negative [positive] for large $|x_{3,i}|$, meaning that $x_{3,i}$ cannot approach ∞ $[-\infty]$. So the maximum of $x_{3,i}$ must be at a critical point, i.e., $\dot{x}_{3,i} = 0$

$$x_{3,i}\big|_{\dot{x}_{3,i}=0} = \frac{r_{3,i}x_{2,i} + \alpha x_{3,i-1}}{r_{4,i}(1 - x_{2,i}) + \alpha}. \tag{11}$$

We see that $x_{3,i}$ is maximized at $x_{2,i} = 1$, $x_{3,i-1} = \mathrm{NH}_{3,\mathrm{max,i-1}}$, yielding

$$\mathrm{NH}_{3,max,\mathrm{i}} = \frac{r_{3,i}}{\alpha} + \mathrm{NH}_{3,max,\mathrm{i-1}}. \tag{12}$$

Letting $x_{3,0} \coloneqq u$ and recursively solving (12) yields (9). □

To establish that $\Omega \subset \mathbb{R}^n$ is positively invariant, we prove that its closure $\bar{\Omega}$ is positively invariant. If $\bar{\Omega}$ is positively invariant then its interior, Ω, is also positively invariant [12].

Proposition IV.2. *The set Ω defined in* (8) *is positively invariant under the dynamics* (3) *for $x(0) \in \Omega$.*

Proof. We prove the proposition by examining $\dot{x}_{j,i}$ on $\partial\Omega$, where $j = 1, 2, 3$ and $i = 1, \ldots, N$. We first examine the lower bound of $x_{3,i}$, $\dot{x}_{3,i}\big|_{x_{3,i}=0} = r_{3,i}x_{2,i} + \alpha x_{3,i-1} \geq 0$. Letting $x_{3,0} \coloneqq u$, we have that $\min_{x_{3,i-1}} \alpha x_{3,i-1} = 0$. Therefore, x_3 cannot cross its lower bound on $\bar{\Omega}$. Since (11) is a critical point and a maximum, x_3 cannot cross its upper bound on $\bar{\Omega}$ and x_3 cannot exit $\bar{\Omega}$. We next examine $x_{1,i}$. First the upper bound, $\dot{x}_{1,i}\big|_{x_{1,i}=d_{max}} = -r_{1,i}d_{max}x_{2,i} - \alpha(d_{max} - x_{i-1}) \leq 0$. Letting $x_{1,0} \coloneqq d$, we have that $\max_{x_{i-1}}(d_{max} - x_{i-1}) = 0$. Therefore, $x_{1,i}$ cannot cross its upper bound on $\bar{\Omega}$. We next examine the lower bound of $x_{1,i}$ $\dot{x}_{1,i}\big|_{x_{1,i}=0} = \alpha x_{1,i-1} \geq 0$. Therefore, $x_{1,i}$ cannot cross its lower bound on $\bar{\Omega}$ and $x_{1,i}$ cannot exit $\bar{\Omega}$. We next examine the bounds of $x_{2,i}$, beginning with the lower bound, $\dot{x}_{2,i}\big|_{x_{2,i}=0} = \beta r_{4,i}x_{3,i} \geq 0$. Therefore, $x_{2,i}$ cannot cross its lower bound on $\bar{\Omega}$. We next examine the upper bound of $x_{2,i}$ $\dot{x}_2\big|_{x_{2,i}=1} = -\beta(r_{2,i} + r_{1,i}x_{1,i} + r_{3,i}) < 0$. Therefore, $x_{2,i}$ cannot cross its upper bound on $\bar{\Omega}$ and $x_{2,i}$ cannot exit $\bar{\Omega}$. Therefore, $\bar{\Omega}$ is positively invariant and so is Ω. □

For technical reasons that will be made clear in Section V-A, we redefine the observation subset to be a closed-set contained in Ω whose boundaries are arbitrarily close to $\partial\Omega$, i.e., if $\delta > 0$ is small, redefine the observation subset to be

$$\Omega_\delta \coloneqq \{x \in \mathbb{R}^n : x_i \in [\underline{x}_i(\Omega) + \delta, \overline{x}_i(\Omega) - \delta], i = 1, \ldots, n\}, \tag{13}$$

which is illustrated in Figure 2, for $N = 1$ $(n = 3)$. Realis-

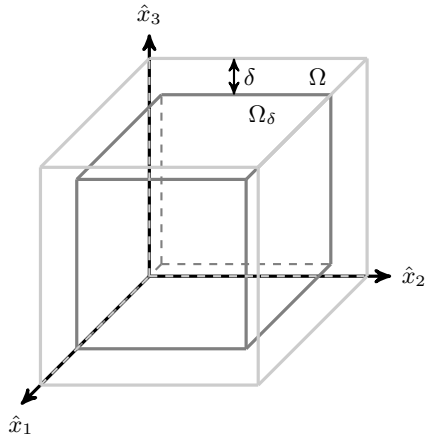

Fig. 2. An illustration of the sets Ω (interior of the light grey polytope), Ω_δ (closure of the dark grey polytope).

tically, the SCR system does not operate on the boundaries of Ω, as this means that the engine is deactivated, no urea is being injected, or large amounts of urea are being injected at low load. We therefore make the following assumption.

Assumption 1. There exists a $\bar{\delta} > 0$ such that for all $\delta \in (0, \bar{\delta})$ the set (13) is non-empty and positively invariant for system (3).

B. Extended Luenberger Hypotheses

To verify the local observability of (3) on Ω_δ, we examine its observability codistribution $d\mathcal{O}(x) := \begin{bmatrix} dh(x) & dL_f h(x) & \cdots & dL_f^{n-1} h(x) \end{bmatrix}^\top$.

We will show that for any number of cells $N > 0$, $d\mathcal{O}(x)$ is full rank on an open and dense subset of Ω_δ. Since the dynamics of (3) differ between $N = 1$ and $N = 2$, we first prove the claim for both $N = 1$ and $N = 2$. In the following discussion, it is assumed that $x(0) \in \Omega_\delta$.

Proposition IV.3. *For $N \in \{1, 2\}$ and any $x \in \Omega_\delta$ the observability codistribution $d\mathcal{O}(x)$ is full rank.*

Proof. Let $N = 1$, $d\mathcal{O}(x)$ is singular if either of $\frac{\partial L_f h(x)}{\partial x_2} = -r_1 x_1$, $\frac{\partial L_f^2 h(x)}{\partial x_3} = \beta r_1 r_4 x_1 (x_2 - 1)$ vanishes. Therefore, observability is lost when $x_1 = 0$ or $x_2 = 1$. These values are not contained in the set Ω_δ, therefore, $d\mathcal{O}(x)$ is full rank on Ω_δ.

The expressions involved in the proof for $N = 2$ are lengthy, so we omit the proof for $N = 2$. □

We now use an induction argument to show that $d\mathcal{O}(x)$ is full rank on an open and dense subset of Ω_δ for any $N > 0$. Since the computational tractability of $d\mathcal{O}(x)$ decreases rapidly with increasing N, we use the method of analysis proposed in [13, Lemma 5]. We first create a copy of (3): $\dot{\bar{x}} = f(\bar{x}) + Bu, \bar{y} = h(\bar{x})$. Defining a state perturbation term $\tilde{x} := x - \bar{x}$ and defining the differential output $\tilde{y} := y - \bar{y}$, we examine the zero-dynamics, i.e., $\tilde{y} = 0$, of the differential-algebraic-system

$$\begin{aligned} \dot{x} &= f(x) + Bu \\ \dot{\tilde{x}} &= f(x) + Bu - f(x - \tilde{x}) - Bu = f(x) - f(x - \tilde{x}) \\ 0 &= h(x) - h(x - \tilde{x}) = \tilde{x}_{1,N}, \end{aligned} \tag{14}$$

which is the difference between (3) and its copy, with equal outputs enforced. If all solutions to (14) require $\tilde{x} \equiv 0$, then (3) is observable. Additionally, if $d\mathcal{O}$ is full rank, then (3) is locally observable and $\tilde{x} \equiv 0$ on the locally observable subset of the state space [13].

Proposition IV.4. *All solutions to* (14) *require $\tilde{x} \equiv 0$.*

Proof. By Proposition IV.3 system (3) is locally observable. Therefore, for $N \in \{1, 2\}$, locally, the only solution to (14) is $\tilde{x} \equiv 0$. As our induction hypothesis, assume that for $N = i - 1 > 2$, the only solution to (14) is $\tilde{x} \equiv 0$. This implies that $\dot{\tilde{x}}_{j,i-1}, \tilde{x}_{j,i-1} = 0, j = 1, 2, 3$.

For (3), it is sufficient to examine $\dot{\tilde{x}}$ and $\tilde{y}$

$$\begin{aligned} \dot{\tilde{x}}_{1,i} &= \tilde{x}_{1,i} r_{1,i} (\tilde{x}_{2,i} - x_{2,i}) - \tilde{x}_{2,i} r_{1,i} x_{1,i} - \alpha(\tilde{x}_{1,i} - \tilde{x}_{1,i-1}) \\ \dot{\tilde{x}}_{2,i} &= -\beta(r_{2,i}(\tilde{x}_{2,i} - x_{2,i}) - r_{1,i}(\tilde{x}_{1,i} - x_{1,i})(\tilde{x}_{2,i} - x_{2,i}) \\ &\quad - r_{4,i}(\tilde{x}_{3,i} - x_{3,i})(\tilde{x}_{2,i} - x_{2,i} + 1) \\ &\quad + r_{3,i}(\tilde{x}_{2,i} - x_{2,i})) - \beta(r_{2,i} x_{2,i} + r_{4,i} x_{3,i}(x_{2,i} - 1) \\ &\quad + r_{3,i} x_{2,i} + r_{1,i} x_{1,i} x_{2,i}) \\ 0 &= \tilde{x}_{1,N}. \end{aligned} \tag{15}$$

We now prove the claim for $N = i$. Since the algebraic constraint $\tilde{x}_{1,N} = 0$ implies that $\dot{\tilde{x}}_{1,N} = 0$, substituting $\dot{\tilde{x}}_{1,i}, \tilde{x}_{1,i}, \tilde{x}_{j,i-1} = 0, j = 1, 2, 3$ into $\dot{\tilde{x}}_{1,i}$ in (15) yields $0 = -\tilde{x}_{2,i} r_{1,i} x_{1,i}$. Since $x_{1,i} > 0$ on Ω_δ, $\tilde{x}_{2,i}$ must be identically 0, implying that $\dot{\tilde{x}}_{2,i} = 0$. With this additional constraint, we solve $\dot{\tilde{x}}_{2,i} = 0$ in (15) for $\tilde{x}_3$, yielding $0 = r_{4,i} \tilde{x}_{3,i} (x_{2,i} - 1)$. Since $x_{2,i} < 1$ on Ω_δ, hence $\tilde{x}_{3,i} \equiv 0$. Therefore $\tilde{x} \equiv 0$ is the only solution to (14) for $N = i$. □

Corollary IV.5. *For any $N > 0$ the SCR system* (3) *satisfies H3, and H1 is satisfied in a neighbourhood of every point in an open and dense subset of Ω_δ.*

Proof. By [13, Lemma 5], the SCR system (3) is locally observable on Ω_δ for any $N > 0$. Furthermore, by [14, Corollary 3.35], $d\mathcal{O}(x)$ is full rank on an open and dense subset of Ω_δ. Since $dT(x) = d\mathcal{O}(x)$, by the inverse function theorem, T is a diffeomorphism in a neighbourhood of every point in an open and dense subset of Ω_δ for any N, thereby satisfying H1 in a neighbourhood of almost every point in Ω_δ. In (14), the $\tilde{x}$ dynamics do not depend on u. This implies that there exists no choice of u for which there are indistinguishable dynamics, therefore H3 is satisfied. □

V. OBSERVERS FOR THE SCR SYSTEM

In this section we define and characterize the dynamics of the proposed observer. The continuous-time dynamics of the observer are defined using the ELO discussed in Section III. By Assumption 1, the states of the SCR system (3) are physically constrained to remain within certain bounds. But the estimates are not constrained to lie within Ω. Thus, we modify the dynamics of the ELO such that when the estimate $\hat{x}(t)$ is on the boundary of Ω_δ, the components of the vector field $\dot{\hat{x}}(t)$ pointing out of Ω_δ are set to 0, thereby preventing the state estimates from leaving Ω_δ. Exponential convergence is guaranteed by switching to the ELO dynamics and estimates if the distance between the two observers exceeds a determined tolerance. Physical intelligibility of the state estimates is attained by applying a projection to the ELO estimates.

A. Extended Luenberger Observer

We construct the observer using a single cell model, i.e., $N = 1$. The vector field of the single cell model is identical to (2). For notational simplicity, we omit the cell index. The diffeomorphism T is given by

$$T(x) = \begin{bmatrix} x_1 \\ -x_1(\alpha + r_1 x_2) \\ x_1(\alpha + r_1 x_2)^2 + \beta r_1 x_1 \gamma(x) \end{bmatrix}$$

where $\gamma(x) \coloneqq (r_2 + r_3 + r_1 x_1)x_2 + (x_2 - 1)r_4 x_3$, and

$$T^{-1}(z) = \begin{bmatrix} z_1 \\ -\frac{z_2+\alpha z_1}{r_1 z_1} \\ \frac{-z_1 z_3 + z_2^2 - \beta\big((r_2+r_3)z_1 z_2 + \alpha r_1 z_1^3 + (\alpha r_2 + \alpha r_3 + r_1 z_2) z_1^2\big)}{\beta r_4 z_1 (z_2 + \alpha z_1 + r_1 z_1)} \end{bmatrix}.$$

Putting the system into the form of (5) by applying $T(x)$ to $f(x)$ in (3), we obtain $\varphi(z) = \text{num}(\varphi(z))/\left(r_1 z_1^2(z_2 + \alpha z_1 + r_1 z_1)\right)$. The functions $T^{-1}(z)$ and $\varphi(z)$ are not well defined at $z_1 = 0$ nor $z_2 = -(\alpha + r_1)z_1$. The former requires $x_1 = 0$ and the latter requires $x_2 = 1$, neither of which are contained in Ω_δ. Therefore, $T^{-1}(z)$ and $\varphi(z)$ are well defined on Ω_δ. Applying T to $g(x) = B$ in (3), we obtain

$$G(z) = \begin{bmatrix} \alpha & 0 \\ \frac{\alpha z_2}{z_1} & 0 \\ \frac{\alpha z_3 - \alpha\beta r_1 z_1 (z_2 + \alpha z_1)}{z_1} & -\alpha\beta r_4 (z_2 + \alpha z_1 + r_1 z_1) \end{bmatrix}. \tag{16}$$

Using the set Ω_δ (13), we can address H2 and H4.

Proposition V.1. *If Assumption 1 holds then the SCR system* (3) *satisfies H2 and H4.*

Proof. Let $\delta \in (0, \bar{\delta})$ and define Ω_δ by (13). This set is compact and positively invariant by assumption, so the states of (3) are confined to a compact set, i.e., the state space of (3) compact, which is sufficient to satisfy H2 [11].

The mapping (16) is locally Lipschitz on Ω and is therefore locally Lipschitz on $\Omega_\delta \subset \Omega$. Since Ω_δ is compact, it follows that (16) is Lipschitz on Ω_δ, satisfying H4. □

Therefore H1–H4 are satisfied and the observer (7) can be constructed for (3) on Ω_δ. The exponential decay of the estimation error $\epsilon \coloneqq \hat{x} - x$ is characterized in [11] by

$$\|\epsilon(t)\| \leq K(\Theta)\exp(-\Theta t/3)\|\epsilon(0)\|, \tag{17}$$

where $K : \mathbb{R}_{>0} \to \mathbb{R}_{>0}$ and $\epsilon(0) \coloneqq \hat{x}(0) - x(0)$.

B. Projected Observer

Although the observer (7) has been shown to be applicable to (3) and, by construction, to be exponentially stable, its state estimates are not necessarily physically meaningful. Given an estimate $\hat{x}$, define the projection

$$\text{proj}(\hat{x}, \Omega_\delta) \coloneqq \arg\min_{p \in \Omega_\delta} \|p - \hat{x}\|, \tag{18}$$

which yields the closest point to $\hat{x}$ on Ω_δ. We propose a "projected observer", constructed by augmenting (7) with a "published estimate" χ. This observer's dynamics are identical to (7), but include the output $\chi = \text{proj}(\hat{x}, \Omega_\delta)$, which is used for feedback control.

In addition to $\text{proj}(\hat{x}, \Omega_\delta)$ always being a physically possible value, it is guaranteed to be at least as good an estimate as $\hat{x}$. Since Ω_δ is convex, the estimate is necessarily improved by replacing it with the closest point in Ω_δ. Hence, the estimation error $\epsilon' \coloneqq \text{proj}(\hat{x}, \Omega_\delta) - x$ of (18) is necessarily smaller than $\epsilon = \hat{x} - x$ for $\hat{x} \notin \Omega_\delta$. Since (18) reduces to $\text{proj}(\hat{x}, \Omega_\delta) = \hat{x}$ for $\hat{x} \in \Omega_\delta$, we have

$$(\forall x \in \mathbb{R}^n)(\forall \hat{x} \in \mathbb{R}^n)(\forall t \geq 0), \epsilon'(t) \leq \epsilon(t). \tag{19}$$

C. Naïve Saturation Implementation

We now characterize a so-called "saturated" observer, whose estimates are denoted by $\hat{x}^\star$, whose estimates are forced to remain in the set Ω_δ. We modify (7) to obtain

$$\begin{aligned} \dot{\hat{x}}^\star(t) &= f(\hat{x}^\star) + B\begin{bmatrix} d & u \end{bmatrix}^\top \\ &\quad - \frac{\partial}{\partial z} T^{-1}(z)\Big|_{z=T(\hat{x}^\star)} S(\Theta)^{-1} C^\top (\hat{x}_1^\star - y) \\ \dot{\hat{x}}_i^\star(t) &= 0, \quad \begin{array}{l} \text{if } \hat{x}_i^\star = \underline{x}_i(\Omega_\delta) \text{ and } \dot{\hat{x}}_i^\star(t) < 0, \\ \text{or } \hat{x}_i^\star = \overline{x}_i(\Omega_\delta) \text{ and } \dot{\hat{x}}_i^\star(t) > 0, i = 1, \ldots, n. \end{array} \end{aligned} \tag{20}$$

If the saturated observer's estimates are in Ω_δ, its dynamics are the same as (7), but augmented with the logic $\dot{\hat{x}}_i^\star(t) = 0$, $i = 1, \ldots, n$ when the estimate is on the boundary of Ω_δ, thereby preventing it from leaving Ω_δ. This modification permits the estimates to "slide" along the boundaries of Ω_δ without crossing over them. A risk of this behaviour is that if $\dot{\hat{x}}_i^\star$ for any i is orthogonal to Ω_δ when $\hat{x}_i^\star$ is saturated and the plant has reached equilibrium, $\hat{x}^\star$ will no longer evolve with time, thereby precluding $\epsilon^\star \coloneqq \hat{x}^\star - x \to 0$ as $t \to \infty$.

Consider the saturated Luenberger observer for the system

$$\begin{aligned} \dot{x} &= \begin{bmatrix} -3 & 1 \\ 1 & -5 \end{bmatrix} x, y = x_1, x(0) = \begin{bmatrix} 1 \\ 2 \end{bmatrix}, \hat{x}(0) = \begin{bmatrix} 0 \\ 0 \end{bmatrix} \\ \Omega_\delta &= \{x \in \mathbb{R}^2 : x_1 \in [-10^{-3}, 1], x_2 \in [-10^{-3}, 2]\}, \end{aligned} \tag{21}$$

with the observer poles placed at $\{-1, -2\}$. As seen in Figure 4, $\hat{x}_1^\star$ does not converge to the equilibrium value $x_1 = 0$, but to 1. Note that in equilibrium that $x = \begin{bmatrix} 0 & 0 \end{bmatrix}^\top$, so the LCx term in the $\dot{\hat{x}}^\star$ dynamics vanishes. The state estimate $\hat{x}^\star$ converges to $\begin{bmatrix} 1 & 0 \end{bmatrix}^\top$. At this point, the vector field is pointing out of Ω_δ, rendering further evolution of $\hat{x}_1^\star$ impossible, thereby precluding convergence.

D. Switching Observer

To address the convergence issue illustrated in Section V-C, we take advantage of the ELO's known error bound (17) and run the ELO in parallel with the saturated observer (20). The proposed observer is of the same form as (20), augmented with a published output as described in Section V-B,

$$\chi(t) = \begin{cases} \hat{x}^\star(t), \text{ if } \|\hat{x}^\star(t) - \hat{x}(t)\| \leq \gamma B(t)\epsilon^\infty \\ \text{proj}(\hat{x}, \Omega_\delta), \qquad \text{otherwise,} \end{cases} \tag{22}$$

where $B(t) \coloneqq K(\Theta)\exp(-\Theta t/3)$, $\hat{x}^\star$ and $\text{proj}(\hat{x}, \Omega_\delta)$ are as defined in (20) and (18), respectively, $\epsilon^\infty \coloneqq \sup_{x \in \Omega_\delta} \|\chi(0) - x\|$, and tuning parameter $\gamma \in \mathbb{R}_{\geq 0}$. Note that $\epsilon^\infty \geq \|\epsilon(0)\|$ for any $x(0), \hat{x}(0) \in \Omega_\delta$.

Theorem V.2. *The estimation error of* (22) *satisfies* $\|\chi(t) - x(t)\| \leq (1 + \gamma)K(\Theta)\exp(-\Theta t/3)\epsilon^\infty$.

Proof. There are two cases in (22). First, we address the case $\chi(t) = \text{proj}(\hat{x}, \Omega_\delta)$. By (17) we have $\|\hat{x}(t) - x(t)\| \leq K(\Theta)\exp(-\Theta t/3)\|\epsilon(0)\| \leq K(\Theta)\exp(-\Theta t/3)\epsilon^\infty \leq (1 + \gamma)K(\Theta)\exp(-\Theta t/3)\epsilon^\infty$, for $\gamma \geq 0$. By (19), we have $\|\chi(t) - x(t)\| = \|\text{proj}(\hat{x}, \Omega_\delta) - x(t)\| \leq \|\hat{x}(t) - x(t)\|$, verifying the theorem in the first case.

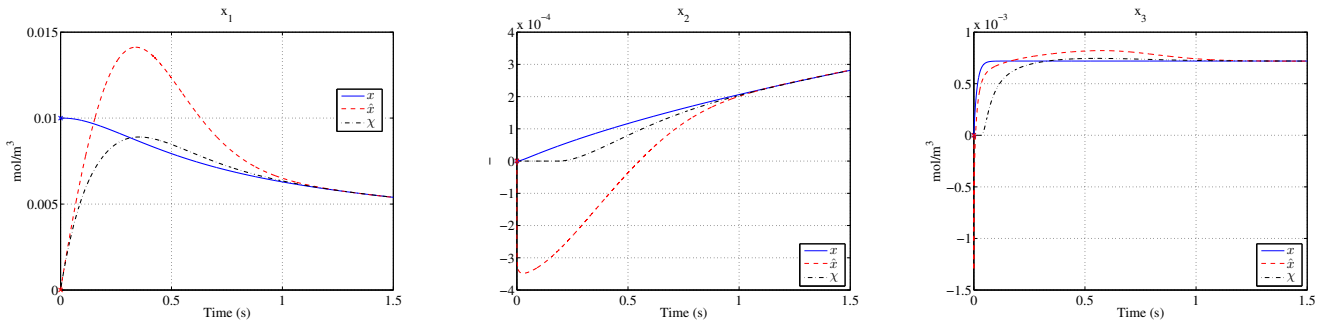

Fig. 3. A comparison of the ELO (7) to the switched observer (22).

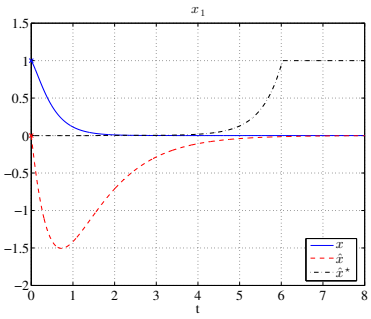

Fig. 4. $x_1(t)$ for the saturated Luenberger observer for system (21).

Second, we address the case $\chi(t) = \hat{x}^\star(t)$. By the triangle inequality $\|\hat{x}^\star(t) - x(t)\| \leq \|\hat{x}^\star(t) - \hat{x}(t)\| + \|\hat{x}(t) - x(t)\|$. Applying (22) and (17) to the first and second right-hand side terms, respectively, we have $\|\hat{x}^\star(t) - x(t)\| \leq \gamma B(t)\epsilon^\infty + B(t)\|\epsilon(0)\| \leq \gamma B(t)\epsilon^\infty + B(t)\epsilon^\infty = (1+\gamma)K(\Theta)\exp(-\Theta t/3)\epsilon^\infty$. □

VI. SIMULATIONS

To illustrate our results, we simulate both the ELO (7) and the switched observer (22) for a single cell engine model. The plant's initial conditions are $x_1(0) = d = 0.01$, $x_2(0) = 0$, $x_3(0) = 0$. We choose $\Theta = 1$, $\alpha = 5$, $\beta = 1/157$, and using the reaction rate parameters from [15], $r_1 = 0.8034$, $r_2 = 0.005885$, $r_3 = 0.6307$, $r_4 = 1.0122 \times 10^4$. A constant $u = 0.01$ is applied at time $t = 0$. Both observers are initialized at $\hat{x}(0) = \chi(0) = \underline{x}(\Omega_\delta)$, with $\delta = 10^{-6}$.

As seen in Figure 3, both observers converge rapidly. However, the ELO's estimates for $\hat{x}_2$ and $\hat{x}_3$ initially take negative values and $\hat{x}_1$ exhibits a relatively high overshoot, exceeding $x_1(0) = d$. Because of the switched dynamics of our proposed observer, χ_2 and χ_3 remain non-negative, which expedites convergence of all three state estimates.

VII. CONCLUSIONS

We introduced a switched nonlinear observer (22) whose dynamics are defined as an augmented version of the observer proposed in [11]; those components of the state estimate's vector field pointing out of an invariant set vanish on the boundary of this invariant set. We showed that the proposed observer is exponentially stable and that the bound on its rate of convergence is the same as that of the observer in [11]. We verified in simulation that the saturation effect can significantly improve the performance of the observer.

REFERENCES

[1] T. V. Johnson, "Diesel Emission Control in Review," in *SAE World Congress & Exhibition*, no. 724. Detroit, MI: SAE, 2006.

[2] M. Koebel, M. Elsener, and M. Kleemann, "Urea-SCR: a promising technique to reduce NOx emissions from automotive diesel engines," *Catalysis Today*, vol. 59, no. 3-4, pp. 335–345, 2000.

[3] T. L. McKinley, "Adaptive Model Predictive Control of Diesel Engine Selective Catalytic Reduction (SCR) Systems," Ph.D. dissertation, University of Illinois at Urbana-Champaign, 2009.

[4] D. Upadhyay and M. Van Nieuwstadt, "Model Based Analysis and Control Design of a Urea-SCR deNOx Aftertreatment System," *Journal of Dynamic Systems, Measurement, and Control*, vol. 128, no. 3, p. 737, 2006.

[5] M. F. Hsieh and J. Wang, "A Two-Cell Backstepping-Based Control Strategy for Diesel Engine Selective Catalytic Reduction Systems," *IEEE Transactions on Control Systems Technology*, vol. 19, no. 6, pp. 1504–1515, 2011.

[6] M. Meisami-Azad, J. Mohammadpour, K. M. Grigoriadis, M. P. Harold, and M. A. Franchek, "PCA-based linear parameter varying control of SCR aftertreatment systems," in *American Control Conference*, San Francisco, CA, USA, 2011, pp. 1543–1548.

[7] M. F. Hsieh and J. Wang, "Nonlinear observer designs for diesel engine selective catalytic reduction (SCR) ammonia coverage ratio estimation," in *Proceedings of the 48h IEEE Conference on Decision and Control*, no. 4, Dec. 2009, pp. 6596–6601.

[8] ——, "Sliding-mode observer for urea-selective catalytic reduction (SCR) mid-catalyst ammonia concentration estimation," *Int. Journal of Automotive Technology*, vol. 12, no. 3, pp. 321–329, 2011.

[9] G. Zhou, J. J. Bagterp, D. Christophe, and J. K. Huusom, "State Estimation in the Automotive SCR DeNO x Process," in *Preprints of the 8th IFAC Symposium ADCHEM*, Singapore, 2012, pp. 501–506.

[10] M. F. Hsieh and J. Wang, "An extended Kalman filter for ammonia coverage ratio and capacity estimations in the application of Diesel engine SCR control and onboard diagnosis," in *American Control Conference*, Baltimore, MD, 2010, pp. 5874–5879.

[11] J. Gauthier, H. Hammouri, and S. Othman, "A simple observer for nonlinear systems applications to bioreactors," *IEEE Transactions on Automatic Control*, vol. 37, no. 6, pp. 875–880, 1992.

[12] H. Amman, *Ordinary Differential Equations: An Introduction to Nonlinear Analysis*. New York, NY: Walter de Gruyter, 1990.

[13] J. A. Moreno, E. Rocha-Cozatl, and A. Vande Wouwer, "Observability/detectability analysis for nonlinear systems with unknown inputs - application to biochemical processes," in *20th Mediterranean Conf. on Control & Automation*, Barcelona, Spain, Jul. 2012, pp. 151–156.

[14] H. Nijmeijer and A. J. van der Schaft, *Nonlinear Dynamical Control Systems*. New York, NY: Springer-Verlag, 1990.

[15] M. Devarakonda, G. Parker, J. H. Johnson, and V. Strots, "Model-based control system design in a urea-SCR aftertreatment system based on NH3 sensor feedback," *International Journal of Automotive Technology*, vol. 10, no. 6, pp. 653–662, 2009.